Factor Va alternative conformation reconstruction using atomic force microscopy.

R C Chaves, S Dahmane, Michaël Odorico, G a F Nicolaes, Jean-Luc Pellequer

Factor Va alternative conformation reconstruction using atomic force microscopy

Rui C. Chaves[1]; Selma Dahmane[1,3]; Michael Odorico[1]; Gerry A. F. Nicolaes[2]; Jean-Luc Pellequer[1,4]

[1]CEA, iBEB, Service de Biochimie et Toxicologie Nucléaire, Bagnols sur Cèze, France; [2]Department of Biochemistry, Cardiovascular Research Institute Maastricht, CARIM, Maastricht University, the Netherlands; [3]Present address: Inserm, Unité 1054, Single Molecule Biophysics Department, Centre de Biochimie Structurale, Montpellier, France; [4]New address: IBS, Univ. Grenoble Alpes/CNRS/CEA, 71 avenue des Martyrs CS 10090, F-38044 Grenoble, Cedex 9, France

Summary

Protein conformational variability (or dynamics) for large macromolecules and its implication for their biological function attracts more and more attention. Collective motions of domains increase the ability of a protein to bind to partner molecules. Using atomic force microscopy (AFM) topographic images, it is possible to take snapshots of large multi-component macromolecules at the single molecule level and to reconstruct complete molecular conformations. Here, we report the application of a reconstruction protocol, named AFM-assembly, to characterise the conformational variability of the two C domains of human coagulation factor Va (FVa). Using AFM topographic surfaces obtained in liquid environment, it is shown that the angle between C1 and C2 domains of FVa can vary between 40° and 166°. Such dynamical variation in C1 and C2 domain arrangement may have important implications regarding the binding of FVa to phospholipid membranes.

Keywords

Coagulation factors, imaging, phospholipids, protein structure / folding, atomic force microscopy

Correspondence to:
Jean-Luc Pellequer
IBS, Univ. Grenoble Alpes/CNRS/CEA
71 avenue des Martyrs CS 10090 F-38044 Grenoble
Cedex 9, France
E-mail: jlpellequer@cea.fr

Financial support:
This work was initially supported by the Agence Nationale de la Recherche [ANR-07-PCVI-0002–01] and the Commissariat à l'énergie atomique et aux énergies alternatives (CEA).

Received: June 1, 2014
Accepted after major revision: July 15, 2014
Epub ahead of print: September 4, 2014

http://dx.doi.org/10.1160/TH14-06-0481
Thromb Haemost 2014; 112: 1167–1173

Introduction

Activation of fibrin is the result of several processes known as the blood coagulation cascade (1–3) which can be activated by two ways: contact activation (the intrinsic pathway); or through tissue factor (the extrinsic pathway). Both lead to the activation of factor X (FXa), then FXa together with the activated factor V (FVa) promotes the conversion of prothrombin to thrombin which in turn catalyses the conversion of fibrinogen to fibrin. The procoagulant prothrombinase complex composed of FVa, FXa, phospholipids and calcium is a key complex that increases the activation of prothrombin by five orders of magnitude (4). Anticoagulation is mediated by activated protein C (APC) which proteolyses FVa (5, 6) which results in a loss of FVa cofactor activity. A frequently occurring single mutation (G1691A) at a codon coding for Arg506 (7), one of the two most important APC cleavage sites in FVa, results in a FV which is resistant to APC. This characteristic gave to FV the highest risk of hereditary venous thrombotic disorder, being up to 15% in the general population of Caucasian origin. The sequence of human FV consists of a single-chain of 2196 residues organised in six domains: A1–A2–A3–B–C1–C2, with the large B-domain being released upon activation of FV to FVa (8). The crystal structure of full FV is still unknown while an A2-less structure of bovine FVa has been obtained (9) (Protein Data Bank [PDB] code: 1SDD). FVa C1 and C2 domains are known to bind phospholipids as demonstrated by site-directed mutagenesis studies (10–12). Thus, the orientation of C1 and C2 domains within FVa is critical for optimal function of the prothrombinase complex.

In the absence of high resolution human FVa structures, FVa models were built (PDB code 1FV4) (13) based on ceruloplasmin (14) and on the binding domain of galactose oxidase (15, 16). With the knowledge of the crystal structure of human FV C2 domain (17), updated models were built (18–20). Further modelling lead to building and simulation of the prothrombinase complex (19, 21). Recently, a crystal structure of the *Pseudonaja textilis* propseutarin C (not activated) has been determined (PDB code 4BXS, [22]). Activated pseutarin C is a homologous to the complex of human FVa and FXa (part of the prothrombinase complex) and is capable of efficient thrombin generation in the absence of membranes. Homologous snake factor V adopts a similar domain conformation to that observed for A2-less structure of bovine FVa (22). As most multi-domain proteins, FVa is likely not adopting a single "rigid" conformation as observed from crystallography

studies but rather is made of a set of possible arrangements which we refer as "conformational variability". Such variability is easier to observe at the single molecule level such as cryo-electron microscopy (EM) (23, 24) or atomic force microscopy (AFM) (25–28). Both approaches can provide information that allows assessment of the global shape of individual molecules which can be used to decrypt the variability of the FVa 3D structure. One of the major differences between cryo-EM and AFM is the signal over noise ratio which is exceptional for the latter since a single image can provide all the useful information (no averaging for AFM). Another distinction between these techniques is that cryo-EM obtains three-dimensional maps whereas AFM can only access to two-dimensional surfaces. Both techniques do not require staining molecules, special orientations of single molecules, or ultra-pure solutions. However, when compared with high-resolution structural biology techniques such as X-ray crystallography and nuclear magnetic resonance that usually obtain resolution better than 3 Å, the estimated resolution in AFM and cryo-EM images is usually above 1 nm. Application of single molecule techniques such as AFM or Cryo-EM are extremely useful to study alternative conformation pathways by looking at one molecule at a time. Because there is no synchronisation of structural conformation, single isolated molecule studies may provide valuable information about the extent of conformational variability of flexible molecules such as those encountered in blood coagulation.

Here, we provide experimental information about the shape of human FVa in solution obtained by AFM. The application of AFM has several intrinsic advantages such as the possibility of imaging in liquid buffer and the capability of providing images of single isolated molecules without averaging and appropriate image processing (29, 30). For high-resolution imaging of 2D-crystal proteins, a sub-nanometer lateral resolution is commonly observed (31) whereas Angstrom-level vertical resolution (height) is classically obtained with AFM imaging (32). FVa has a molecular weight of ~173 kDa with a molecular size estimated as 12×9×5 nm^3 and thus is perfectly amenable to high-resolution AFM imaging. In this study, AFM images of FVa were obtained in liquid environment and were used to reconstruct the 3D structure of complete FVa by assembling the A trimer structure to the two C domains. Reconstructed FVa models were compared with two available models of FVa: 1FV4 available in PDB (13) and named here FVa2000; and the most recent model (20) named here FVa2007 which is mostly based on the crystal structure 1SDD (9) (►Figure 1 and Suppl. Figure 1, available online at www.thrombosis-online.com).

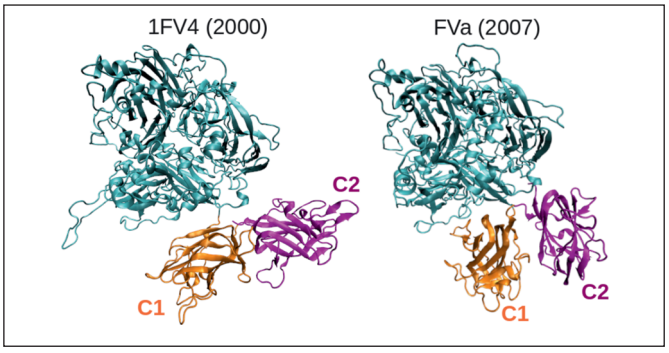

Figure 1: Ribbon representation of two FVa three-dimensional models. The A trimer is drawn in cyan and the C1 and C2 domains are drawn in orange and magenta, respectively. On the left, the original model is presented with a colinear arrangement between C1 and C2 domains (13). On the right, a revised model of FVa (20) based on the A2-less crystal structure of bovine FVa (9) is shown in which the C1 and C2 long axes appear parallel.

Materials and methods

FVa protein

The preparation of purified FVa was obtained from human plasma following the procedure described in Nicolaes et al. (6). The protein was >99% pure as judged by SDS-PAGE analysis.

AFM image

Activated factor V was imaged in buffer using a multimode V AFM with the PeakForce mode (Bruker AXS). Scan rate was set at 1 Hz. The ScanAsyst software was used only to control the gain; all other ScanAsyst parameters were manually controlled. The peak force ramp was set to 25 nm and all other peak force parameters were set as default. During imaging, the peak force set point was manually adjusted to obtain the best visual imaging at the lowest imaging force. Cantilevers OTR8 (k=0.57 N/m, Bruker AFM Probes) with a nominal tip radius of 2 nm were used. FVa (9 nM) was inserted in a drop of 50 µl HEPES buffer (20 mM, 150 mM NaCl, pH 7.1) on a mica substrate pretreated with $MgCl_2^+$ (20 mM) for 1 hour (h) at 25°C. FVa molecules were not completely fixed and thus some molecules moved during imaging. Thus, it was not possible to zoom several times of the same region and we collected raw images at the resolution of 9.75 Å/px as defined by a scan size of 1.0 × 1.0 μm^2 with 1024 × 1024 px^2 (►Figure 2).

FVa molecules lie down with a "flat-on" orientation where the pseudo-trimeric axis of the A domains is perpendicular to the mica surface. This orientation allows the imaging of all the domains of FVa. Although this orientation is very convenient for AFM imaging, the orientation of FVa is unlikely to be similar when bound to phospholipids (13, 19, 22, 24). Attempts to image FVa molecule of phospholipids with AFM were unsuccessful, so far.

The raw image was treated with DeStripe (33) for stripe noise reduction and 20 objects were randomly selected (►Figure 2 and Suppl. Figure 2, available online at www.thrombosis-online.com). The average height of these objects was 9.0 nm (range from 6.4 to 11.6 nm without considering spurious artifacts). Images of selected objects were eroded individually to reduce the tip dilation effect, using a theoretical tip diameter of 2 nm and side wall angles of 15° (34). As a comparison of the tip-dilation effect, a "3D" convoluted image of FVa has been computed using the Adepth server (35) with a grid size of 2 Å and a grid boundary of 50 Å (►Figure 3). Despite current available tools, dilation/erosion of single isolated proteins in AFM images remains challenging. A possibility to

circumvent the problem would be to modify the reconstruction protocol to perform docking steps using the experimental dilated topographic surfaces and a similarly dilated surface of 3D structures used as docking units. A similar approach is under investigation (Chaves et al., in preparation). Details for the reconstruction of the complete FVa 3D structure is based on a protocol that is described in the supplementary section.

Results

Single isolated human coagulation factor Va (FVa) were imaged in liquid environment using atomic force microscopy (AFM). AFM topographs of FVa were extracted from data in ►Figure 2. Using the reconstruction protocol described previously, three units of FVa (A trimer and two C domains) were assembled and a sample of multiple conformations for reconstructed FVa is shown in ►Figure 4**.** The reconstruction of FVa molecule has been made in two stages. First, the A trimer, then the C1 and C2 domains, are "docked" independently beneath the experimentally obtained AFM topographic surface (28, 36). Second, the three units (A trimer, C1, and C2) are assembled altogether using a brute force combinatorial approach. Results are scored by the match observed between the experimental AFM topographic surface and the surface of the reconstructed assembly. In addition, top answers do not allow bumps between the three assembled units. In this study, we focused our attention on the particular angle made between C1 and C2 domains (►Figure 5). The reference used here is: an angle of 0° implies that C1 and C2 are collinear whereas an angle close to 180° implies that C1 and C2 are perfectly parallel. More precisely, the angle between C1 and C2 is computed using the following two vectors: v_2 = Asn2036 – Leu1957 (C1 domain), v_3 = Ser2117 – Gly2037 (C2 domain), using Cα atoms coordinates of the corresponding residues.

The C1^C2 angles of the two published FVa models are 131.9° for model FVa2000 and 39.6° for model FVa2007 (►Figure 5). Histogram distribution of C1^C2 angles computed among the twenty assembled FVa models in this study is shown in ►Figure 5 and illustrates a large dynamical range. The average computed C1^C2 = 134.7° with a range from 40.4° to 166.4°. When compared with published FVa models, the C1^C2 orientation in reconstructed FVa as was assessed in the current study is closest to that of the model FVa2000 (►Figure 5).

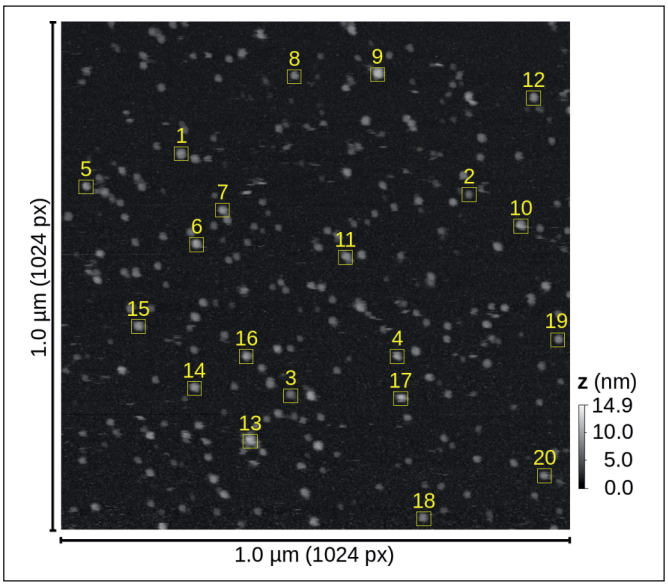

Figure 2: Activated factor V was imaged in liquid using a multimode V AFM with the PeakForce mode (Bruker AXS). The raw image resolution is 9.75 Å/px obtained in a field of 1.0 × 1.0 µm² (1024×1024 px²) and was processed using DeStripe (33). The randomly selected 20 objects are indicated with yellow boxes.

Discussion

Activated coagulation factor V (FVa) requires binding to phospholipid membranes for enhancing the catalytic conversion of prothrombin with factor Xa. Phospholipid membranes concentrate in a two-dimension space the constitutive elements of the prothrombinase complex, thereby increasing the probability of productive collisions and thus enhancing catalytic efficiency (2). It

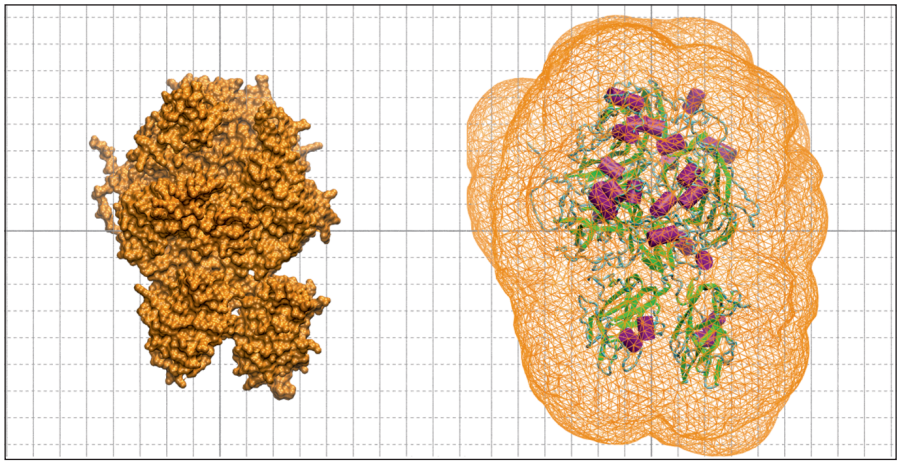

Figure 3: Simulation of a dilation effect of an image of FVa. On the left, the molecular surface of FVa is shown in orange. On the right, at the same scale, the secondary structure of FVa is drawn in ribbon where magenta and green indicate α-helices and β-strands, respectively, loops are coloured in cyan. The pseudo-3D convolution of FVa is represented by the iso-surface of atomic depth (computed using the Adepth server, (35)) shown in orange mesh. The threshold of the iso-surface corresponds to a distance of 2 nm from the surface of the FVa protein. A ruler is drawn in the background where each line is spaced 1 nm from each other. Image built with VMD (38).

has been demonstrated that the FVa C2 domain binds phospholipids (17, 37). However, additional evidences pointed out to other FVa regions involved in phospholipid binding such as the A3 domain (38) and the C1-C2 domains (39). Recently, it was also observed that the C1 domain makes direct contact with phospholipids (11, 40). The partial X-ray structure of bovine FVa suggested that C1 and C2 domains could concomitantly bind to phospholipids due to their side-to-side (parallel) orientation (9). The significant flexibility in C1 and C2 orientation relative to the A-trimer observed from AFM imaging and computational reconstruction suggests that such additional freedom may be involved in optimal membrane binding of C1 and C2, thus allowing faster phospholipid binding. In addition, the flexibility of C1 and C2 participates to the necessary avidity effect of using two or three domains to bind to phospholipids. Coagulation cascade must work quickly and improving membrane affinity by having flexible anchors such as C1 and C2 domains likely enhances constitution of efficient prothrombinase complex. It should be added that the flexibility in the C1-C2 domain could also be important for the proper orientation of FVa towards APC, the central enzyme of the protein C anticoagulant pathway, important for the proteolytic inactivation of FVa.

Are there other supportive evidences of structural variation in C1-C2 orientation? The recently determined structure of pro-pseutarin C, which is homologous to human FV and FX, contains domains A1-A3 as well as domains C1 and C2 (22). Using equivalent vector assignments, the C1^C2 angle in pro-pseutarin C is 66°. This angle value is intermediate between the two alternative conformations presented in models FVa2000 and FVa2007 (▶Figure 5). Although the difference in C1^C2 angle in pseutarin C relative to FVa models is likely due to a local sequence variation, both C1 and C2 domains of pseutarin C are expected to bind phospholipids and consequently, the variability in C1^C2 angle could also be interpreted in term of structural variability in phospholipid binding. Beside pseutarin C, there is a homologous coagulation factor VIIIa (FVIIIa) in which two complete X-ray crystal structures indicate a parallel orientation of C1 and C2 domains (41, 42). When using cryo-electron microscopy with the coagulation FVIIIa light chain bound to a single bilayer lipid nanotube, a three-dimensional reconstruction revealed a similar collinear arrangement of C1 and

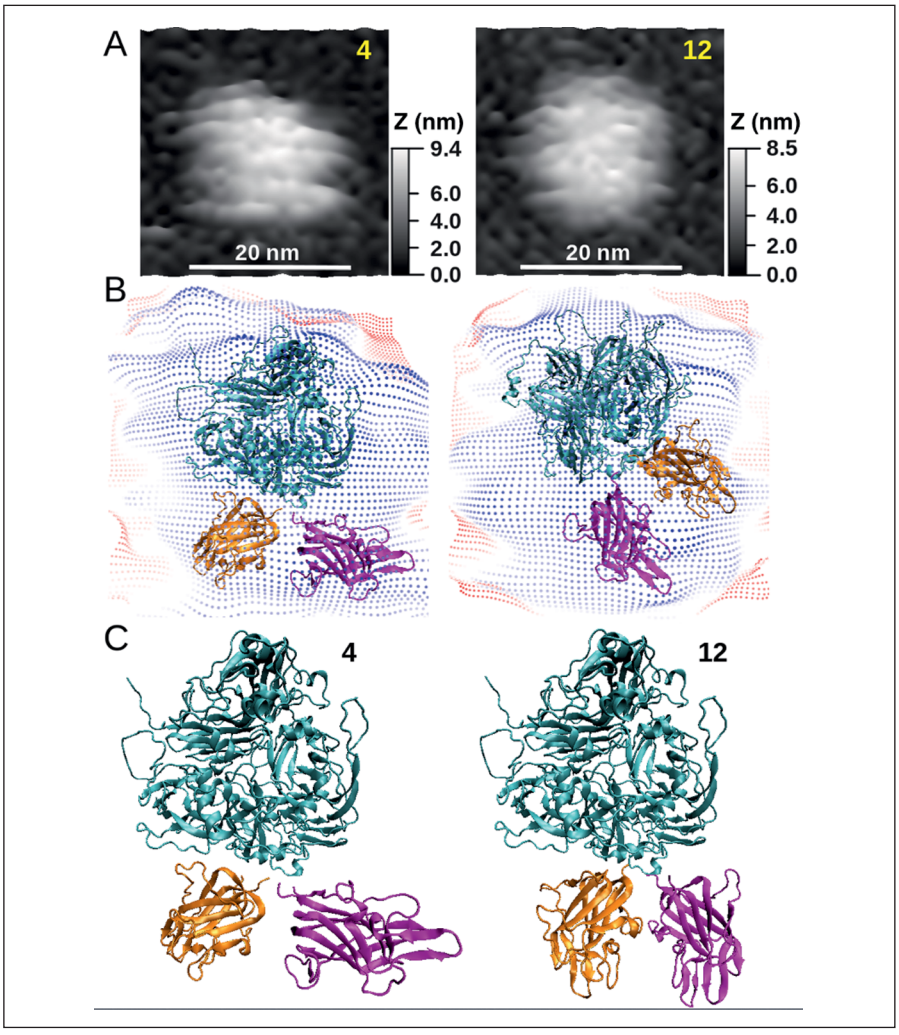

Figure 4: Top solution from the AFM-Assembly protocol for two representative reconstructions (#4 and #12) out of the 20 objects considered in Figure 2. The C1 and C2 domains are organised on the left according to a collinear arrangement and on the right according to a parallel side-to-side arrangement. A) AFM topographic surface is shown. B) A top side view of the reconstruction of FVa docked beneath the AFM surface topography represented with blue and red dots. C) Example of final reconstruction models #4 and #12 based on AFM topographic images where the A trimer is drawn in cyan, and the C1 and C2 domains are drawn in orange and magenta, respectively. Surface images performed with VMD (48).

C2 domains (v_2^v_3 = 152.2°) (43). Such a value is closely related to the average 134.7° observed in FVa reconstruction from our study.

A selection of 20 protein topographs has been made from a single AFM imaging experiment (Suppl. Figure 2, available online at www.thrombosis-online.com). Is a single AFM image enough? To obtain a high-quality AFM topograph in liquid, several concomitant conditions must be met. First, molecules must be well adsorbed on the mica substrate; second, the AFM tip must have an optimally thin apex (a few nanometers) and not be worn; third, the imaging parameters must be optimally set so that the force exerted on the molecules must be small enough not to denature them but high enough to obtain a good resolution. Ideal conditions to obtain high-resolution AFM images are difficult to obtain from single isolated molecules (44). Thus, as long as the above conditions are met, having a single AFM image does allow for the production of reliable AFM topographs. In addition, the physical dimension of FVa obtained by AFM is compatible with that obtained from X-ray crystallography when taking the dilation effect into account.

Twenty topographic surfaces (crops) were analysed. Their selection had been made randomly. Additional crops could have been added to the list. However, the redundancy observed in our results convinced us that no additional crops were required. Although the computational time for each crop is reasonable (about 24h CPU), the amount of data generated by the protocol is huge when assuming high-resolution docking as performed in this study (9 10^{11} docking results to manage per run). Because only AFM topographic surfaces are used in the reconstruction protocol, there is always a "surface limitation": information is only available for domains that are accessible to the AFM tip. Consequently, when two domains overlap, it is not possible to distinguish the domain underneath, and thus, our current reconstruction protocol only targets "flat-on" oriented single molecules.

For single isolated molecules, as opposed to molecules organized in 2D arrays, the main image distortion besides that from the piezoelectric ceramics of AFM is the dilation of molecules due to the finite size of the AFM tip. In short, what is recorded in the AFM topograph is the shape of the molecule of interest plus the contribution of the AFM tip. Thus, we observed protein topographs that have sizes larger than expected by simply taking size information obtained from X-ray crystallography. For instance, 3D structure of FVa indicates that the size of the molecule is 12×9 nm² (▶Figure 3) but the average diameter measured from AFM topograph is closer to an average of 21×18 nm² (standard deviation for the 20 selected objects is 2 nm). By simulating a pseudo 3D tip convolution effect using the Adepth server (35) on the 3D structure of FVa, a convoluted size of 16×13 nm² was obtained (▶Figure 3) using a putative tip radius of 2 nm (which is among the thinnest tip size we can obtain at this time). Note that if the tip radius is increased to 4 nm, the convoluted size of FVa would be 20×17 nm². It should be noted that the dramatic effect of convolution is essentially located on the edge of the image. In the case of FVa, since the AFM imaging is mostly performed on a "flat-on" orientation, the central section of AFM topograph has minimal convolution artifact and the docking of atomic structure is correct.

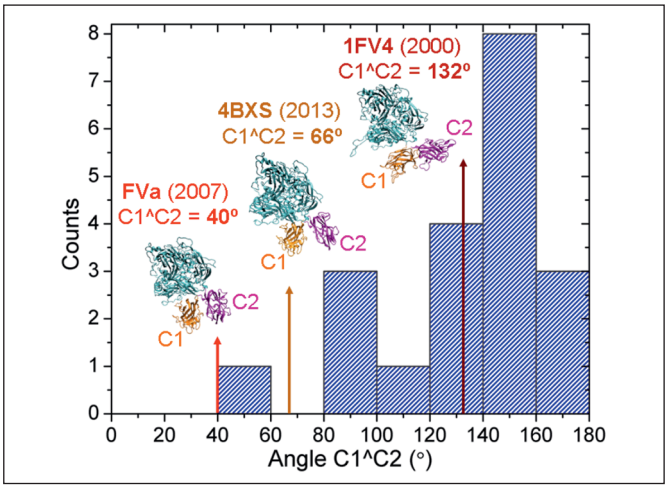

Figure 5: Angle C1^C2 distribution for the experimentally-assembled structures represented as blue shaded histograms. Angles for models FVa2000 and FVa2007 are represented by the red arrows and correspond to values 131.9° and 39.6°, respectively. Angle for the C1^C2 propseutarin C structure (a recently determined FVa crystal structure from snake venom) is 65.8° and was computed with v_2 = Glu1271 – Leu1191 (C1 domain), v_3 = Thr1351 – Gly1272 (C2 domain).

Finally, the similarity between the longest dimension of dilated 3D structure of FVa (16 nm) and that obtained in AFM topograph (19 nm) suggest that physical molecules on mica are FVa and that their structure/size is close to the native state based on crystallographic data.

The AFM topograph of isolated FVa molecules has been obtained with a sampling resolution of 9.75 Å/px. The resolution extension to 2.4 Å/px (see Suppl. Material, available online at www.thrombosis-online.com) obtained with Gwyddion is useful for computational purposes but does not improve the signal present in the native experimental image. Is this original sampling resolution enough? Is it possible to interpret AFM topograph at such a sampling resolution? To simplify the discussion, let's assume that the sampling resolution is 1 nm/px. What is the limiting factor? In this work, the relative orientation of C1 and C2 domains is analysed. Both C1 and C2 domains have an equivalent size of 3×4 nm² or an equivalent of 12 pixels. The FVa A domains have an equivalent size of 8×9 nm² or 72 pixels (▶Figure 3). Thus, the assembly made in this work consists in making the difference of 24 pixels out of 72 (~33%). Therefore, despite the relatively low sampling resolution (~1 nm/px) which does not allow the delineation of atomic structures from the observed AFM topograph, it is reasonable to assume that domains of different sizes from a single molecule could be distinguished.

What is the relevance of computed angles in FVa reconstructions? Does the assembly protocol converges toward a unique solution or does it provide spurious results? To answer this question, let's look at the convergence. RMSDs have been computed for the top 100 assemblies relative to the top 1 answer for each of the 20 AFM topographs. Median RMSD values have been computed for the top 10, top 20… top 100 assemblies for each topograph. For

What is known about this topic?

- The structure of factor Va (FVa) is made by an assembly of two domains (A, and C), forming an heavy chain (A1-A2) and a light chain (A3-C1-C2) in which three structural units can be defined (A1-A2-A3 or A trimer, C1 and C2).
- A partial X-ray crystal structure is known for the bovine FVa where the A2 domain is missing and a homologous inactivated prothrombinase complex from snake.
- Comparative models of complete human FVa structures are available, most recent ones are based upon the incomplete structure of bovine FVa.

What does this paper add?

- This paper presents high-resolution AFM topography of single isolated human FVa in liquid environment.
- Reconstruction with the three structural units (A trimer, C1 and C2 domains) to assemble complete human FVa.
- Results indicate that there is a significant variability in the orientation of C1 and C2 domains which could bring significant highlight in FVa phospholipid binding.

the 20 AFM topographs, the average of each median values has been plotted as a function of the ranking (Suppl. Figure 4, available online at www.thrombosis-online.com). A linear tendency is clearly observed (r^2=0.977) and indicates that the top 10 assemblies resemble more the top 1 assembly than does the top 100 assemblies. If the median value is computed for only the top 10 assemblies, we observed an average RMSD median value of 4.5 Å across the 20 selected topographs. As a comparison, when the core structures of both models (FVa2007 and FVa2000) are superimposed using sup3d (45), the global RMSD of the backbone of all residues is about 13 Å (Suppl. Figure 1, available online at www.thrombosis-online.com). These results suggests that assembly made with AFM topograph are convergent toward a limited number of solution that shows a variation of about 4.5 Å which is much less than the difference between the two competitive models of FVa. Nevertheless, despite the observed convergence, there is no unique solution of docking three units of FVa in AFM topographs. It should be reminded that the C1-C2 angle is not measured directly from the AFM topograph, but only after the three-dimensional reconstruction of full FVa molecules. Thus, despite the precision obtained from each reconstruction, the accuracy depends on the reconstruction quality. But, we are confident that reconstructed FVa molecules using AFM topographs are representative of true structural variability observed when FVa is deposited on mica. These results taken altogether suggest that there is flexibility in the C1-C2 orientation and that this variability can be captured when analysing dynamical behavior of single individual macromolecules (46).

Conclusions

Results from the 20 reconstructed FVa structures obtained from AFM images of individual FVa molecules indicate that the orientation between the C1 and C2 domains agrees predominately with the FVa2000 model. Results do not imply that the FVa2000 model is correct or that the model FVa2007 is incorrect; instead given the fact that AFM is able to sample the thermal motion in biomolecules, we believe that our results indicate that both models represent extreme snapshots of what could be the conformational variability of FVa C domains. More generally, conclusions from single isolated molecule images and full structure reconstruction may provide important information on the dynamics of the orientation of C1 and C2 domains which may have in turn important implications regarding phospholipid binding.

Acknowledgements

We thank Jean-Marie Teulon, Yannick Delcuze and Pierre Parot for their support on AFM imaging, Shu-wen W. Chen for image processing developments, and we thank Arnaud Martel (CEA/DSV/iBITEC-S, Saclay) for his help on setting up the websites. Tools to perform this analysis are available online: DockAFM, http: //biodev.cea.fr/dockafm (47) and CombineDocksAFM, http: //biodev.cea.fr/combinedocksafm (this work).

Conflicts of interest

None declared.

References

1. Davie EW, Ratnoff OD. Waterfall sequence for intrinsic blood clotting. Science 1964; 145: 1310–1312.
2. MacFarlane RG. An enzyme cascade in the blood clotting mechanism, and its function as a biochemical amplifier. Nature 1964; 202: 498–499.
3. Dahlback B. Blood coagulation. Lancet 2000; 355: 1627–1632.
4. Esmon CT, Suttie JW, Jackson CM. The functional significance of vitamin K action. Difference in phospholipid binding between normal and abnormal prothrombin. J Biol Chem 1975; 250: 4095–4099.
5. Kalafatis M, Rand MD, Mann KG. The mechanism of inactivation of human factor V and human factor Va by activated protein C. J Biol Chem 1994; 269: 31869–31880.
6. Nicolaes GAF, Tans G, Thomassen MCLGD, et al. Peptide bond cleavages and loss of functional activity during inactivation of factor Va and factor VaR506Q by activated protein C. J Biol Chem 1995; 270: 21158–21166.
7. Bertina RM, Koeleman BPC, Koster T, et al. Mutation in blood coagulation factor V associated with resistance to activated protein C. Nature 1994; 369: 64–67.
8. Jenny RJ, Pittman DD, Toole JJ, et al. Complete cDNA and derived amino acid sequence of human factor V. Proc Natl Acad Sci USA 1987; 84: 4846–4850.
9. Adams TE, Hockin MF, Mann KG, et al. The crystal structure of activated protein C-inactivated bovine factor Va: Implications for cofactor function. Proc Natl Acad Sci USA 2004; 101: 8918–8923.
10. Nicolaes GA, Villoutreix BO, Dahlback B. Mutations in a potential phospholipid binding loop in the C2 domain of factor V affecting the assembly of the prothrombinase complex. Blood Coagul Fibrinolysis 2000; 11: 89–100.
11. Saleh M, Peng W, Quinn-Allen MA, et al. The factor V C1 domain is involved in membrane binding: identification of functionally important amino acid residues within the C1 domain of factor V using alanine scanning mutagenesis. Thromb Haemost 2004; 91: 16–27.

12. Peng W, Quinn-Allen MA, Kane WH. Mutation of hydrophobic residues in the factor Va C1 and C2 domains blocks membrane-dependent prothrombin activation. J Thromb Haemost 2005; 3: 351–354.
13. Pellequer JL, Gale AJ, Getzoff ED, et al. Three-dimensional model of the coagulation factor Va bound to activated protein C. Thromb Haemost 2000; 84: 849–857.
14. Villoutreix BO, Dahlback B. Structural investigation of the A domains of human blood coagulation factor V by molecular modeling. Protein Sci 1998; 7: 1317–1325.
15. Pellequer J-L, Gale AJ, Griffin JH, et al. Homology models of the C domains of blood coagulation factors V and VIII: A proposed membrane binding mode for FV and FVIII C2 domains. Blood Cells Mol Dis 1998; 24: 448–461.
16. Villoutreix BO, Bucher P, Hofmann K, et al. Molecular models for the two discoidin domains of human blood coagulation factor V. J Mol Model 1998; 4: 268–275.
17. Macedo-Ribeiro S, Bode W, Huber R, et al. Crystal structures of the membrane-binding C2 domain of human coagulation factor V. Nature 1999; 402: 434–439.
18. Orban T, Kalafatis M, Gogonea V. Completed three-dimensional model of human coagulation factor Va. Molecular dynamics simulations and structural analyses. Biochemistry 2005; 44: 13082–13090.
19. Autin L, Steen M, Dahlback B, et al. Proposed structural models of the prothrombinase (FXa-FVa) complex. Proteins 2006; 63: 440–450.
20. Gale AJ, Yegneswaran S, Xu X, et al. Characterization of a factor Xa binding site on factor Va near the Arg506 APC cleavage site. J Biol Chem 2007; 282: 21848–21855.
21. Lee CJ, Lin P, Chandrasekaran V, et al. Proposed structural models of human factor Va and prothrombinase. J Thromb Haemost 2008; 6: 83–89.
22. Lechtenberg BC, Murray-Rust TA, Johnson DJ, et al. Crystal structure of the prothrombinase complex from the venom of Pseudonaja textilis. Blood 2013; 122: 2777–2783.
23. Zhou ZH. Towards atomic resolution structural determination by single-particle cryo-electron microscopy. Curr Opin Struct Biol 2008; 18: 218–228.
24. Stoilova-McPhie S, Parmenter CD, Segers K, et al. Defining the structure of membrane-bound human blood coagulation factor Va. J Thromb Haemost 2008; 6: 76–82.
25. Shao Z. Probing nanometer structures with Atomic Force Microscopy. News Physiol Sci 1999; 14: 142–149.
26. Scheuring S, Boudier T, Sturgis JN. From high-resolution AFM topographs to atomic models of supramolecular assemblies. J Struct Biol 2007; 159: 268–276.
27. Muller SA, Muller DJ, Engel A. Assessing the structure and function of single biomolecules with scanning transmission electron and atomic force microscopes. Micron 2011; 42: 186–195.
28. Chaves RC, Teulon J-M, Odorico M, et al. Conformational dynamics of individual antibodies using computational docking and AFM. J Mol Recognit 2013; 26: 596–604.
29. Fechner P, Boudier T, Mangenot S, et al. Structural information, resolution, and noise in high-resolution atomic force microscopy topographs. Biophys J 2009; 96: 3822–3831.
30. Chen S-wW, Odorico M, Meillan M, et al. Nanoscale structural features determined by AFM for single virus particles. Nanoscale 2013; 22: 10877–10886.
31. Schabert FA, Engel A. Reproducible acquisition of Escherichia coli porin surface topographs by atomic force microscopy. Biophys J 1994; 67: 2394–2403.
32. Binnig G, Quate CF, Gerber C. Atomic force microscope. Phys Rev Lett 1986; 56: 930–933.
33. Chen S-wW, Pellequer JL. DeStripe: frequency-based algorithm for removing stripe noises from AFM images. BMC Struct Biol 2011; 11: 7.
34. Trinh M-H, Odorico M, Bellanger L, et al. Tobacco mosaic virus as an AFM tip calibrator. J Mol Recognit 2011; 24: 503–510.
35. Chen S-wW, Pellequer JL. Adepth: new representation and its implications for atomic depths of macromolecules. Nucl Acids Res 2013; 41: W412-W416.
36. Trinh M-H, Odorico M, Pique ME, et al. Computational reconstruction of multidomain proteins using atomic force microscopy data. Structure 2012; 20: 113–120.
37. Ortel TL, Devore-Carter D, Quinn-Allen MA, et al. Deletion analysis of recombinant human factor V. Evidence for a phosphatidylserine binding site in the second C-type domain. J Biol Chem 1992; 267: 4189–4198.
38. Kalafatis M, Jenny RJ, Mann KG. Identification and characterization of a phospholipid-binding site of bovine factor Va. J Biol Chem 1990; 265: 21580–21589.
39. Kalafatis M, Rand MD, Mann KG. Factor Va-membrane interaction is mediated by two regions located on the light chain of the cofactor. Biochemistry 1994; 33: 486–493.
40. Majumder R, Quinn-Allen MA, Kane WH, et al. A phosphatidylserine binding site in factor Va C1 domain regulates both assembly and activity of the prothrombinase complex. Blood 2008; 112: 2795–2802.
41. Ngo JC, Huang M, Roth DA, et al. Crystal structure of human factor VIII: implications for the formation of the factor IXa-factor VIIIa complex. Structure 2008; 16: 597–606.
42. Shen BW, Spiegel PC, Chang CH, et al. The tertiary structure and domain organization of coagulation factor VIII. Blood 2008; 111: 1240–1247.
43. Stoilova-McPhie S, Lynch GC, Ludtke S, et al. Domain organization of membrane-bound factor VIII. Biopolymers 2013; 99: 448–459.
44. Schneider SW, Larmer J, Henderson RM, et al. Molecular weights of individual proteins correlate with molecular volumes measured by atomic force microscopy. Pflugers Arch 1998; 435: 362–367.
45. Chen S-wW, Pellequer JL. Identification of functionally important residues in proteins using comparative models. Curr Med Chem 2004; 11: 595–605.
46. Bongini L, Fanelli D, Piazza F, et al. Freezing immunoglobulins to see them move. Proc Natl Acad Sci USA 2004; 101: 6466–6471.
47. Chaves RC, Pellequer JL. DockAFM: benchmarking protein structures by docking under AFM topographs. Bioinformatics 2013; 29: 3230–3231.
48. Humphrey W, Dalke A, Schulten K. VMD: visual molecular dynamics. J Mol Graph 1996; 14: 33–38.